Approaches to the Determination of the Three-dimensional Architecture of Ribosomal Particles

A. YONATH,*† K.R. LEONARD,‡ S. WEINSTEIN,*§ AND H.G. WITTMANN§

*Department of Structural Chemistry, Weizmann Institute of Science, Rehovot, Israel;
†Max-Planck Research Unit for Structural Molecular Biology, Hamburg, Federal Republic of Germany;
‡European Molecular Biology Laboratory, Heidelberg, Federal Republic of Germany;
§Max-Planck Institute for Molecular Genetics, West Berlin (Dahlem)

The intricate and accurate process of biosynthesis of protein molecules occurs in a similar manner on ribosomes of all organisms. Ribosomes consist of two subunits that associate upon initiation of protein biosynthesis. Each subunit is a structurally defined assembly of proteins and RNA chains with a characteristic sedimentation coefficient (e.g., 30S and 50S for the small and the large ribosomal subunits from bacteria). During the last two decades a vast amount of information has been accumulated about the function and the chemical, biological, and genetic properties of ribosomes (for review, see Chambliss et al. 1979; Wittmann 1982, 1983; Hardesty and Kramer 1986). This knowledge has shed light on the entire process of protein biosynthesis, although the understanding of the detailed mechanism of this process is still severely limited by the lack of a molecular model.

As objects for crystallographic studies, ribosomal particles are of enormous size, with no internal symmetry. Furthermore, they are unstable and flexible. Therefore, even the first necessary step of these studies, namely crystallization, seemed, until recently, to be a formidable task. Despite that, a systematic exploration of crystallization conditions supported by development of innovative experimental techniques for fine control of the volume of the crystallization drops, as well as for sophisticated seeding (Yonath et al. 1982a; Yonath and Wittmann 1987a,b), led to reproducible production of crystals of intact ribosomal particles.

Bacterial ribosomes were chosen because they are well characterized biochemically, they can be prepared in high purity and large amounts, and they provide a system that is independent of in vivo events. Thus, the natural capacity of eukaryotic ribosomes to form two-dimensional sheets, stuck to cell membranes (e.g., Milligan and Unwin 1986), has been extended by us to a higher degree of organization, expressed in vitro. As a result, three-dimensional crystals and two-dimensional sheets of intact ribosomal particles from *Escherichia coli*, *Bacillus stearothermophilus*, *Thermus thermophilus*, and *Halobacterium marismortui* have been obtained (Table 1 and Yonath et al. 1980, 1982b, 1983a,b, 1984, 1986a,b,c, 1987; Wittmann et al. 1982; Yonath 1984; Shevack et al. 1985; Wittmann and Yonath 1985; Piefke et al. 1986; Shoham et al. 1986; Makowski et al. 1987; Yonath and Wittmann 1987a,b,c). Currently, crystals grow from virtually every preparation of large ribosomal particles from *B. stearothermophilus* and *H. marismortui*, but, because of the intricate nature of the particles, the exact conditions for the growth of well-ordered and large crystals must still be slightly varied for each ribosomal preparation. Moreover, the quality of the crystals depends, in a manner not yet fully characterized, on the procedure used in preparing the particles and on the bacterial strain. There is a strong correlation between crystallizability and biological activity of all our crystallization systems. So far, inactive ribosomal particles could not be crystallized. Moreover, in spite of the natural tendency of ribosomes to disintegrate, all crystallized particles retain their biological activity, even for several months, in contrast to the short lifetime of isolated ribosomes in solution. This property accords well with the hypothesis that when external conditions (e.g., hibernation) demand prolonged storage of potentially active ribosomes in living organisms, temporary periodic organization occurs in vivo.

Synchrotron radiation provides the most intense, well-collimated X-ray beam. It is essential for crystallographic data collection from crystals of ribosomal particles due to their large unit cell dimensions (Table 1), their fragility, and their sensitivity. Until recently, all our crystallographic studies, including the assessment of the quality of the crystals and the determination of the resolution limits and the unit-cell parameters, had to be carried out solely with synchrotron radiation. The newly developed method of crystallographic data collection at cryotemperature (Hope 1985) paved the way for conducting preliminary experiments with less powerful X-ray sources, such as rotating anodes.

Phase information is essential for maturation of crystallographic studies. We are currently attempting to determine phases by both conventional and novel heavy-atom techniques. A great advantage for the production of heavy-atom derivatives is the large variety of ribosomal components and the wide spectrum of materials that interact specifically with these components (e.g., antibiotics; for review, see Nierhaus and Witt-

Table 1. Packing Parameters of Two- and Three-dimensional Crystals of Ribosomal Particles

Source	Crystal form	Cell Dimensions, (Å) determined by electron microscopy	X-ray crystallography
70S *E. coli*	A[a]	340 × 340 × 590; 120°; P6	
70S *Bacillus stearothermophilus*	2D[b], AS[a]	200 × 440; 93°	
50S *Halobacterium marismortui*	1, P[a]	310 × 350; 105°	
	2, P	148 × 186; 95°	147 × 181; 97°
	3, P	170 × 180; 75°	214 × 300 × 590; $C222_1$
50S *Bacillus stearothermophilus*	1, A	130 × 254; 95°	
	2, A	156 × 288; 97°	
	3, A	260 × 288; 105°	
	4, A	405 × 405 × 256; 120°	
	5, A	213 × 235 × 315; 120°	
	6[c], A	330 × 670 × 850; 90°	360 × 680 × 920; $P2_12_12_1$
	2D, A	145 × 311; 108°; P2	
	2D, AS[a]	148 × 360; 109°; P1	

[a]Crystals are grown by vapor diffusion from alcohols or their mixtures (A), polyethylene glycol (P), or by mixing with ammonium sulfate (AS).

[b]All forms, unless marked 2D, are three-dimensional crystals. 2D = two-dimensional sheets.

[c]Same form and parameters for crystals of the large ribosomal subunits of – L11 mutant of the same source.

mann 1980). In favorable cases, derivatives can be used for an unambiguous localization of specific ribosomal components. Results of electron microscopy may also contribute toward phase determination. The model of the particle under study, obtained at medium resolution by three-dimensional image reconstruction of two-dimensional sheets, could be placed in the crystallographic unit cell using crystal-packing information derived from the electron micrographs of thin sections of the investigated crystal (Leonard et al. 1982). This, together with information obtained from crystallographic studies of isolated individual ribosomal components at high resolution (Leijonmarck et al. 1980; Appelt et al. 1981; Wilson et al. 1986), can be used for iterative phase determination by molecular replacement methods, assuming that the conformations of crystallized isolated components are similar to their conformations within the ribosome.

EXPERIMENTAL PROCEDURES

Ribosomes and their subunits were prepared and their integrity and activity were checked as described (Arad et al. 1987b; Yonath and Wittmann 1987a). Procedures for the production of three-dimensional crystals and two-dimensional sheets, the crystallographic data collection, and the three-dimensional image reconstruction are described in detail (Yonath et al. 1982a, 1986c; Arad et al. 1984, 1987b; Piefke et al. 1986; Makowski et al. 1987; Yonath and Wittmann 1987a,b,c). All crystallographic studies reported here have been performed using synchrotron radiation, at 4°C and −180°C (Hope 1985).

Radioactive *N*-ethylmaleimide was reacted with ribosomal particles to determine the accessibility of sulfhydryl groups of ribosomal proteins of the 50S subunits from *B. stearothermophilus* and *H. marismortui*. For the latter, this procedure was also used to locate these groups, since the sequence of only a few proteins from this source is known.

A gold cluster and its radioactive derivative were prepared following basically a known procedure (Bartlett et al. 1978). Functional groups were attached to the gold clusters for covalent binding to ribosomal particles through accessible sulfhydryl groups (S. Weinstein and W. Jahn, in prep.). The extent of binding of the gold cluster was determined by measuring the radioactivity associated with the 50S particles, as well as by neutron activation (performed at Soreq Nuclear Research Laboratories, Israel). The proteins that bind *N*-ethylmaleimide were identified by locating the radioactivity on a two-dimensional gel electropherogram of the ribosomal proteins.

RESULTS AND DISCUSSION

Three-dimensional Image Reconstruction

The large size of ribosomal particles, which is an obstacle for crystallographic studies, permits their direct investigation by electron microscopy. Thus, in the case of intact ribosomal particles, a combination of X-ray crystallography with electron microscopy and three-dimensional image reconstruction should be possible and is expected to provide a powerful tool for our studies. Using electron microscopy, the initial steps of crystallization can be detected and the tendency of crystallization of native and modified particles can be followed rather quickly, in contrast to the long time

needed for the growth of large three-dimensional crystals. Results from electron microscopy can also be used to locate and orient the particles within the crystallographic unit cells, and models obtained by three-dimensional image reconstruction may facilitate extraction of phase information. Thus, structure determination by three-dimensional image reconstruction from two-dimensional sheets is justified not only in its own right, but also because of its expected contribution to the determination of phases needed for crystallographic analysis. Therefore, we have pursued, side by side, X-ray crystallography using three-dimensional crystals and three-dimensional image reconstruction from two-dimensional sheets.

We have developed two procedures for the growth of two-dimensional sheets of ribosomal particles: (1) in hanging drops from alcohols (AL) (Arad et al. 1984); and (2) on flat surfaces using mixtures of salts and alcohols (ST) (Piefke et al. 1986; Arad et al. 1987 and in prep.; Yonath et al. 1987). These sheets were negatively stained with either gold-thioglucose or uranyl acetate and used for three-dimensional image reconstruction studies.

Gold-thioglucose is an inert stain and is expected to reveal the outer contour of the particles. Additional information may be obtained from sheets stained with uranyl acetate. This stain is chemically reactive; thus along with its ability to elucidate the external contour of the particle, it may interact with the negatively charged components of the ribosomal particles (most likely the rRNA). The extent of this interaction is somewhat irregular, since it depends on the accessibility of the appropriate components and may be influenced by irregularities of the electron microscopy grid. In general, the resolution and the quality of sheets that have been negatively stained by uranyl acetate are lower than those of sheets stained by gold-thioglucose. In favorable cases the influence of the staining procedure is minimal. An example may be the tunnel of the large ribosomal subunits (see below). It is resolved in all reconstructions of the two-dimensional sheets of 50S subunits from *B. stearothermophilus*, independent of the staining material (Yonath et al. 1987), as well as in the reconstructed model of the unstained sheets from chick embryos (Milligan and Unwin 1986).

***The two-dimensional sheets of 70S particles from* B. stearothermophilus.** These are built of dimers, packed in relatively small unit cells: $190 \pm 15 \times 420 \pm 15$ Å, $\gamma = 107° \pm 3°$ (Fig. 1). Optical diffraction patterns of electron micrographs of negatively stained specimens with uranyl acetate and of cross-linked sheets stained with gold-thioglucose extend to 40 Å and 47 Å, respectively.

Eleven reconstructions of sheets from three different preparations have been performed. The resulting model of the ribosomal particle (Fig. 1) has average dimensions similar to those determined by other physical methods (Wittmann 1983). On the basis of the known molecular weight of the 70S particle (2.3×10^6) and of the volume obtained from the three-dimensional image reconstruction, the calculated density of the particle is 1.3–1.4 g/cm^3, and the V_m for a hypothetical crystal of the thickness of the sheets (about 200 Å) is 2.6–2.7 Å^3/dalton.

Several features were revealed by the analysis (Fig. 1) of models derived from the gold-thioglucose-stained sheets. The two ribosomal subunits are arranged around an empty space of a volume of $4 \times 10^5 \pm 2 \times 10^5$ Å^3. This space is large enough to accommodate most of the components of protein biosynthesis. There are variations in the size of this space as revealed in different reconstructions. This may result from sheets, built of ribosomes that may carry some components of protein biosynthesis, such as tRNA or fractions of mRNA.

Because only a small fraction of the particles in the drop actually consists of two-dimensional sheets, they could not be separated from the rest of the drop. Therefore, we tested the migration profile on sucrose gradients of the ribosomal particles in the crystallizing drops. It was found that particles subjected to crystallization conditions comigrate with standard particles.

The two ribosomal subunits are fairly separated. Only the two ends of the small subunit are in contact with the large subunit. The sum of the contact areas is 400–800 Å^2. The overall shapes of both subunits have been compared with models that have previously been suggested for these particles. There is a similarity between the model of the small subunit obtained by visualization of single particles (Wittmann 1983) and that revealed by our studies. Isolated 30S particles seem to be wider than the reconstructed ones within the 70S particles. This may be a consequence of the contact of the isolated particles with the flat electron microscope grid. In contrast, particles within the crystalline sheets are held together by their interactions with the 50S particles as well as by interparticle crystalline forces. These construct a network that may stabilize the conformation of the particles and decrease, or even eliminate, the influence of the flatness of the grids. The portion of the reconstructed 70S particle that we assigned as the large subunit may be correlated to the image of this subunit as revealed in our previous studies (Fig. 2 and Yonath et al. 1987), both at 28 Å (the actual resolution of the studies) and at 55 Å.

Reconstruction of models of 70S ribosomes from sheets stained with uranyl acetate led to a model that shows the features described above, as well as regions where uranyl acetate, acting as a positive stain, was incorporated into the particle. This may indicate that in these regions the RNA is concentrated and/or easily exposed to the stain. Such regions could be located on the surface of the large subunit where it faces the internal empty space. Penetration of uranyl acetate to the region assigned as "collar's ridge" on the small subunits was also detected. In both cases, the staining of these areas with uranyl acetate may stem either from the existence of exposed rRNA regions, as previously found (Milligan and Unwin 1986), or from the presence of mRNA and tRNA in these locations.

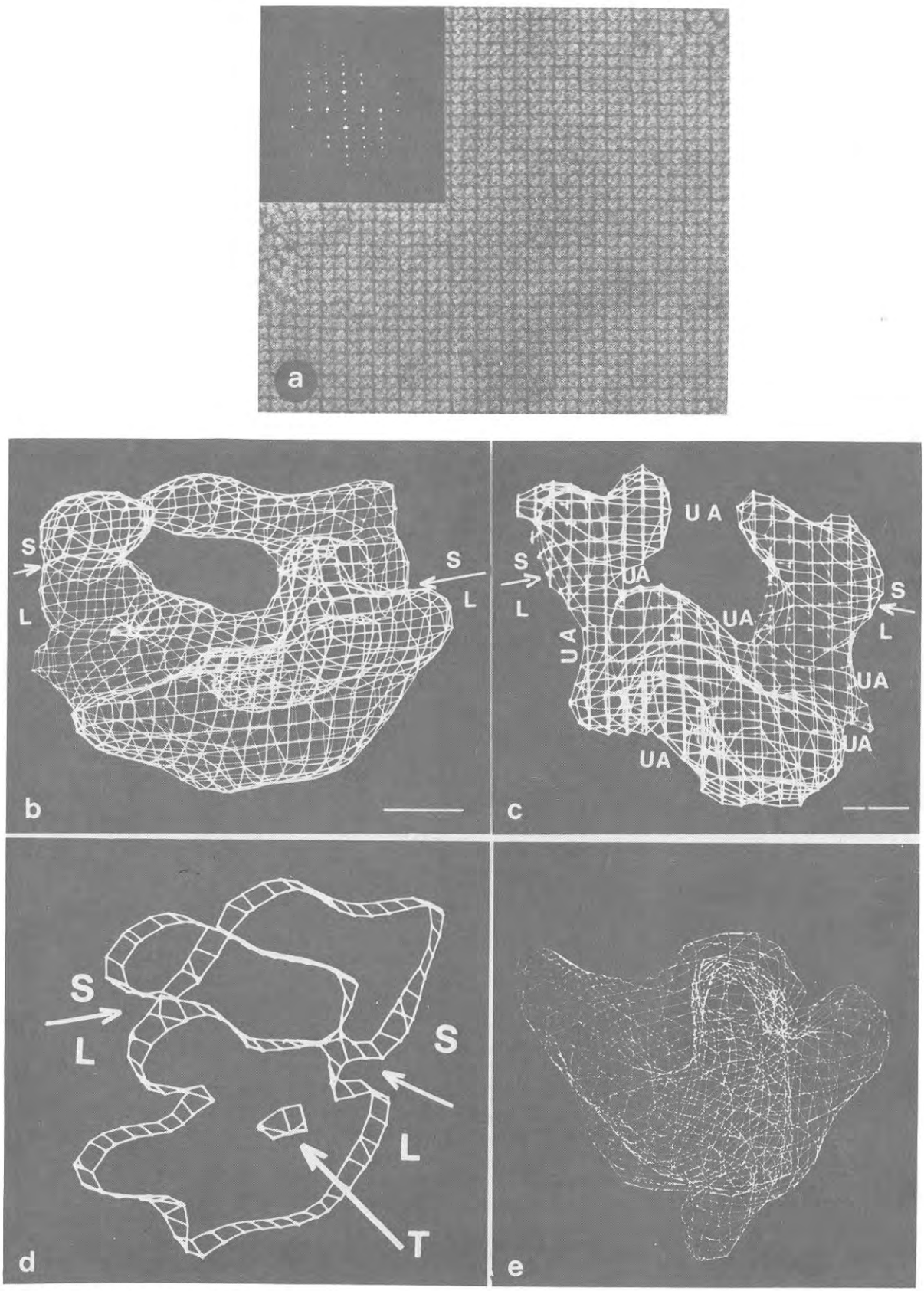

Figure 1. (*See facing page for legend.*)

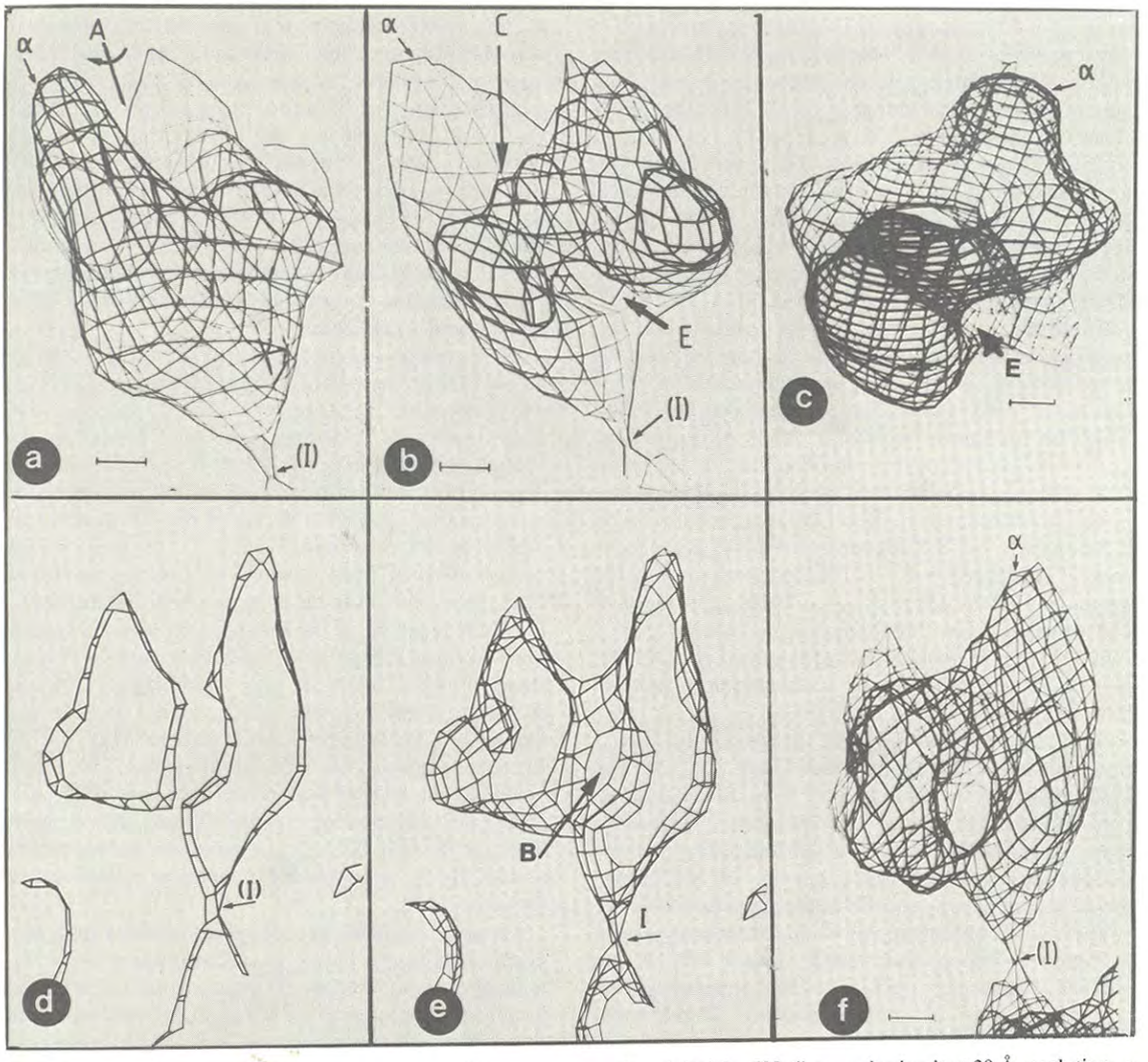

Figure 2. Computer graphic display of the outline of the reconstructed model of the 50S ribosomal subunit at 30 Å resolution. α marks the longest arm. E is the exit site. (*a*) A side view of the model. The entire particle and part of a second one are shown. The arrow (I) points at the crystal contact between the two particles. A marks the approximate axis around which the model was turned to obtain the view shown in *b*. Bar length=20 Å. (*b*) The model shown in *a* rotated about the A axis. C points at the cleft between the projecting arms, at the site it turns into the tunnel. (*c*) A view into the tunnel from the cleft. (*d*) The outline of a 20-Å-thick section in the middle of the reconstructed model, showing that the tunnel spans the particle. (*e*) The outline of a 40-Å-thick section in the middle of the reconstructed model. The branching of the tunnel is seen (B). (*f*) The model viewed into the branch of the tunnel from the exit point.

Figure 1. Computer graphic display of the outline of the reconstructed model of the 70S ribosome at 47 Å resolution. (*a*) Image of a two-dimensional sheet (× 28,000) of 70S particles from *B. stearothermophilus*, stained by gold-thioglucose, and an optical diffraction pattern from an area containing about 20 × 15 unit cells. (*b*) Computer graphic display of the outline of the reconstructed model of the 70S ribosome at 47 Å resolution, stained with gold-thioglucose. L and S indicate the 50S and the 30S subunits, respectively. The arrows point at the interface between the two subunits. Bar length=20 Å. (*c*) Computer graphic display of the outline of the reconstructed model of the 70S ribosome at 42 Å resolution stained with uranyl acetate, at a similar orientation to that shown in *b*. UA shows the regions to which uranyl acetate binds. L and S indicate the 50S and the 30S subunits. The arrows point at the interface between the two subunits. Bar length=20 Å. (*d*) The outline of a 20-Å-thick section in the middle of the reconstructed model of the 70S ribosome. T indicates part of the tunnel. (*e*) The 30 Å resolution reconstructed model of the 50S subunit, obtained as in Fig. 2, viewed in a projection which resembles models derived from electron microscopy studies of single particles.

The model for the 50S subunits. This was reconstructed at 30 Å resolution. Two-dimensional sheets of these particles from *B. stearothermophilus* have been obtained from three different preparations using both above mentioned procedures. In all cases the sheets consist of small unit cells (e.g., $145 \pm 10 \times 311 \pm 20$ Å, $\gamma = 108 \pm 3°$ for the AL sheets). These cell dimensions are close to those of forms 1 and 2 of three-dimensional crystals of the same particles (Table 1 and Yonath 1984). Both AL and ST are well ordered, and optical diffraction patterns of electron micrographs of negatively stained specimens extend to 30 Å and 28 Å, respectively. In both cases each unit cell contains two particles with dimensions similar to those obtained by other methods (for reviews, see Chambliss et al. 1979; Wittmann 1982, 1983; Hardesty and Kramer 1986). Based on the known molecular weight of this particle (1.6×10^6 daltons), and on the thickness of the sheets (160–170 Å), as determined by the three-dimensional image reconstruction studies, the calculated density of a 50S particle is 1.3–1.4 g/cm^3, and the V_m for a hypothetical crystal is 2.6–2.7 Å^3/dalton. Both are in good agreement with values tabulated by Matthews (1968) and calculated for three-dimensional crystals of 50S subunits from *H. marismortui* (Makowski et al. 1987), as well as for other large nucleoprotein structures (Hogle 1982; Richmond et al. 1984).

Interparticle contacts within the sheets are clearly revealed in our three-dimensional map (Fig. 2). The best-defined contact area is 5–12 Å in diameter, compatible with the regular intermolecular interactions found in crystals of proteins or nucleic acids. As these dimensions are beyond the resolution of our studies, the nature of these contacts cannot be identified.

The main features revealed by our analysis are shown in Figure 2. The particle has a concave surface that consists of several protrusions 25–30 Å in diameter, the approximate size of globular proteins of molecular weights typical of many ribosomal proteins. A long arm is located on one side of the particle (bottom of the particle shown in Fig. 2). Several projecting arms, two of which are longer than the others, are arranged radially around the other edge (upper side of the particle shown in Fig. 2), near the presumed interface with the 30S subunit (Fig. 1). A narrow elongated cleft is formed between the projecting arms and turns into a tunnel of a diameter of up to 25 Å and a length of 100–120 Å. This tunnel is present in all reconstructions of the ST sheets, independent of the staining material, as well as in reconstructed 80S ribosomes from chick embryos (Milligan and Unwin 1986). In every reconstructed particle there is a region of low density that branches off the tunnel to form a Y (or V) shape, and terminates on the other side of the particle (Fig. 2). As yet, we cannot determine the exact nature of this region. It may be a loosely packed protein region, but in some reconstructed models the density of the branch is so low that it appears as a branch of the main tunnel.

The functional significance of the tunnel is still to be determined. Originating at the presumed site for actual protein biosynthesis and terminating on the other end of the particle, and being of a diameter large enough to accommodate even the largest amino acids, this tunnel appears to provide the path taken by the nascent polypeptide chain. Furthermore, this tunnel is of a length that could accommodate and protect from proteolytic enzymes a peptide of about 40 amino acids in an extended conformation (Malkin and Rich 1967; Blobel and Sabatini 1970; Smith et al. 1978). It remains to be seen whether the tunnel terminates at a location compatible with that assigned by immunoelectron microscopy as the exit site for the growing polypeptide chain (Bernabeau and Lake 1982).

We have also reconstructed a model using a selected subset of diffraction data at lower resolution (55 Å). At this resolution the particle is almost spherical and shows only two thick and short arms instead of the elongated arms resolved in the 30 Å resolution studies. This accords well with the shape of the portion of the reconstructed model (at 47 Å) of the 70S particle assigned as the 50S subunit (Fig. 1), as well as with models derived from electron microscopy studies of single particles. It should be mentioned that the tunnel is clearly resolved in the low-resolution reconstructed model of the 50S particle, whereas in the 70S reconstructed particle there are only some indications for its existence. Thus, a portion of the tunnel could be detected in a section through the particle (Fig. 1). As mentioned above, the 70S particles were harvested while active, and it is feasible that nascent protein chains are still attached to a part of them. It is conceivable that the tunnel is only partially resolved due to this and/or to the intrinsic low resolution of this reconstruction.

Several models for 50S ribosomal subunits were suggested previously, based on electron microscopic visualization and averaging of single particles. Our model is more similar to those that have no flat surfaces and to those in which the projecting arms are arranged radially. It can be positioned so that its projected view resembles the usual image seen when single particles are investigated by electron microscopy (Fig. 1e). In addition, there are a few filtered images of two-dimensional sheets tilted by certain angles, which show the same shape and include the characteristic features that have been visualized by electron microscopy of single particles (Fig. 3). At the same time, there are some discrepancies in the nature of the gross structural features between our model and the others, which, as in the case of the 70S particles, probably stem from the basic differences between visualization of isolated particles in projection and the inherently more objective character of structure analysis by diffraction methods.

As mentioned above, the resolution of the sheets stained with uranyl acetate is somewhat lower (32–35 Å) than that of the sheets stained with gold-thioglucose. Consequently, the reconstructed model shows less detail. However, the essential features—the concave shape, the tunnel, and the projecting arms—are resolved. Comparison of this model with that obtained

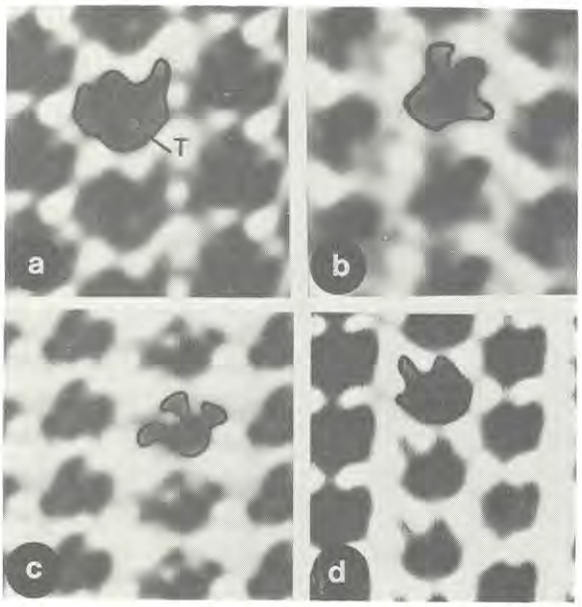

Figure 3. Filtered images of electron micrographs of sheets of 50S subunits from *B. stearothermophilus* in which the depicted view resembles that derived from electron microscopy of single particles. (*a*) AL sheets stained with uranyl acetate. The tunnel T can be detected. Tilt of 25°. (*b–d*) ST sheets stained with gold thioglucose. Tilts of 35°, 20° and 30°, respectively.

from the same sheets stained with gold-thioglucose shows regions (on one of the long arms, on the body of the particle, and near the interface with the 30S) where uranyl acetate, acting as a positive stain, is incorporated into the particle. This may indicate that in these regions the rRNA is concentrated and/or easily exposed to the stain.

There is a significant shortening of the long projecting arms in models reconstructed from sheets grown from alcohols. This may indicate that the arms are positioned firmly in an environment of salts, but may flex when exposed to alcohols. Inherent flexibility of the long arms has been observed also in reconstruction of rotated single particles (Verschoor et al. 1985).

Assignment of the known functional domains of 70S particles and of 50S subunits to the various structural features still awaits further investigations. In view of the recent progress of our crystallographic studies and of our ability to reproducibly produce two-dimensional sheets of native as well as modified ribosomal particles, we are hopeful that we shall be able to locate specific sites on a detailed model in the foreseeable future.

Crystallographic Studies

The process of crystal growth is initiated by nucleation. Although many biological molecules and complexes have been crystallized, little is known about the mechanism of nucleation. Most of the data currently available concerning the process of nucleation of crystals of biological systems are based on rather indirect evidence, such as monitoring aggregation under crystallization conditions by scattering techniques. Crystals of ribosomal particles provided an excellent system for direct investigation of nucleation. In our experimental setup, the crystallization process was interrupted before the formation of mature crystals, and the crystallization medium was examined by electron microscopy. It was found that the first step in crystal growth is unspecific aggregation and that nucleation starts by a rearrangement within the aggregates (Yonath et al. 1982b).

Crystallographic studies are currently being performed on crystals from the large ribosomal subunits from *B. stearothermophilus* and *H. marismortui*. Two crystal forms of 50S subunits from *B. stearothermophilus* have been grown. The first are obtained directly in X-ray capillaries at 4°C by vapor diffusion from mixtures of methanol and ethylene glycol as long pointed needles that may reach the size of $1.5 \times 0.3 \times 0.2$ mm (Fig. 4). Since most of them grow with one of their faces adhering to the walls of the capillaries, it was possible to irradiate them without removing the original growth solution. This is essential since any handling of these crystals is virtually impossible. Although most of the crystals grow with their long axes parallel to the capillary axis, a fair number grow in different directions. Thus, using synchrotron radiation, it was possible to determine the unit cell constants ($360 \times 680 \times 920$ Å) of an orthorhombic form ($P2_12_12_1$) and to obtain diffraction patterns from all the zones (Fig. 4) without manipulating the crystals (Yonath et al. 1984, 1986c). A fair amount of crystallographic data to 18 Å resolution has been collected from these crystals.

Several diffraction patterns of single crystals as well as those of samples containing large numbers of microcrystals of this form include oriented arcs and distinct spots, with spacings similar to those measured from diffuse diffraction patterns of ribosome gels and extracted rRNA (Klug et al. 1961; Langridge and Holmes 1962) and extending to 3.5 Å. For aligned crystals the average arc length is 60°. Such patterns may arise from partial orientation of the nucleic acid component within the particle.

Recently, a second form of crystals from this source has been obtained. Here the growth solution contains polyethylene glycol, magnesium chloride, and ammonium sulfate. Crystals of this form grow within 10–14 days at 4°C, appear as polygons, and reach a maximum size of $0.1 \times 0.1 \times 0.1$ mm. Extensive attempts to increase their size by seeding have been, so far, unsuccessful.

Crystals of the 50S subunits from *H. marismortui* grow as thin plates at 19°C by vapor diffusion from polyethylene glycol in the presence of salts that mimic, to some extent, the composition of the natural environment of these bacteria, the Dead Sea. Although fragile, these crystals can be manipulated. Thus, seeding was used for obtaining larger (maximum size $0.6 \times 0.6 \times 0.2$ mm) as well as more ordered crystals (Fig. 5). We have taken advantage of the major role played by the Mg^{++} concentration in crystallization of ribosomal particles.

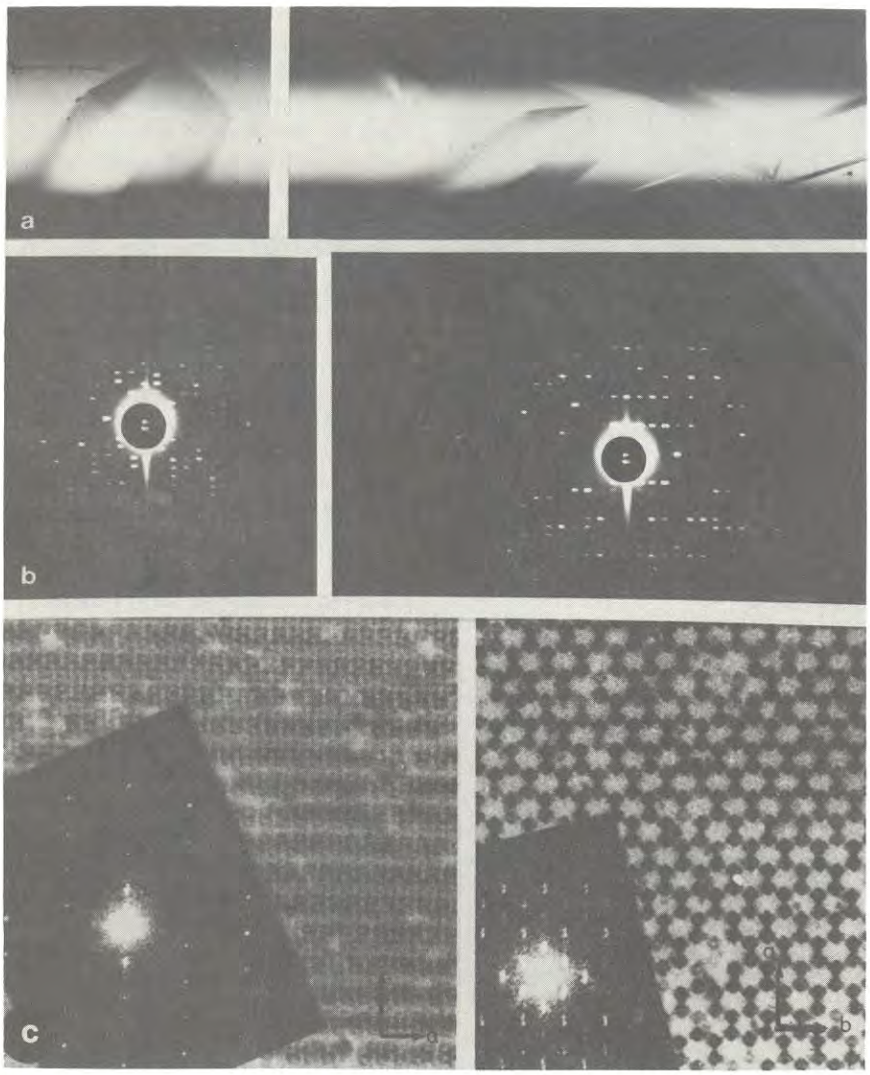

Figure 4. (*a*) Crystals of the 50S ribosomal subunits from *B. stearothermophilus* grown in 0.5-mm X-ray capillaries by vapor diffusion at 4°C. Crystallization mixture of 20 μl 50S ribosomal subunits (10–20 mg/ml) in H-I buffer (Yonath et al. 1980), 0.01 M spermine, 1% methanol, and 10 mM HEPES or glycine buffer (pH 8.4) was equilibrated with a reservoir of 12% methanol, 12% ethylene diol, and 0.5 M $NaCl_2$, pH 8.4. (*b*) X-ray diffraction patterns from crystals similar to those shown in *a*, obtained at −4°C with synchrotron radiation (A1 station at CHESS/CORNELL Univ. operating at 5 GeV, current 30–40 mA) with 0.3 mm collimated X-ray beam with wavelength of 1.55 Å, on a HUBER precession camera equipped with a He path. Exposure time 3 min, crystal to film distance 200 mm. (*Left*) 1° rotation photograph of Ok1 zone, 680 × 920 Å. (*Right*) 0.4° rotation photograph of hk0 zone, 360 × 680 Å. (*c*) Electron micrographs of positively stained (2% uranyl acetate) thin sections of crystals similar to those shown in *a* that have been fixed in 0.2% glutaraldehyde and embedded in resin ERL 4206. Optical diffraction patterns are inserted. (*Left*) Section approximately perpendicular to that shown on the right. Repeat distances measured from optical diffraction: 330 × 1050 Å. This corresponds to the h01 zone (360 × 920 Å) in the X-ray patterns. (*Right*) Micrograph showing the characteristic open packing of this crystal form. The orthogonal choice of axes corresponds to the 680 × 920 Å zone observed in the X-ray diffraction patterns. Lattice spacing calculated from optical diffraction: 670 × 850 Å.

It was found that three-dimensional crystals of 50S ribosomal subunits from *B. stearothermophilus* grow in relatively low Mg^{++} concentration, whereas the production of two-dimensional sheets requires a high Mg^{++} concentration, at which growth of three-dimensional crystals is prohibited. Similarly, for spontaneous crystal growth of 50S subunits from *H. marismortui*, the lower the Mg^{++} concentration is, the thicker the crystals are. With these points in mind, a variation of the standard seeding procedure has been developed. Thin crystals of the 50S subunits from *H. marismortui* grown spontaneously under the lowest possible Mg^{++} concentration are transferred to mixtures in which the Mg^{++} concentration is so low that the transferred crystals almost dissolve, but after several days new microcrystals can be observed. These reach their maximum size after 3–4 weeks, are 10–30-fold thicker than the original seeds, are very well ordered, and diffract to a resolution of 5.5 Å (Fig. 6). They have relatively small unit cells of 214 × 300 × 584 Å ($C222_1$), which

are compactly packed, in contrast to the open structure of the large crystals of *B. stearothermophilus* (Fig. 4).

Between −2°C and 4°C, these crystals are rather stable in the synchrotron beam. However, their higher resolution diffraction terms decay within the first few minutes. Thus only 1–3 rotation patterns could be taken from an individual crystal, and more than 260 crystals were needed to collect an entire data set. Recently, we have shown that at −180°C, irradiated crystals hardly show radiation damage for days. Thus, for the first time, a full data set could be collected from a single crystal. Moreover, under these conditions, the life expectation of the crystals is long enough to allow X-ray diffraction experiments using rotating anodes as X-ray generators. Thus, initial parameters such as quality of crystals, their resolution, unit cell constants, and isomorphism may be determined at conventional X-ray diffraction laboratories, and the progress of the struc-

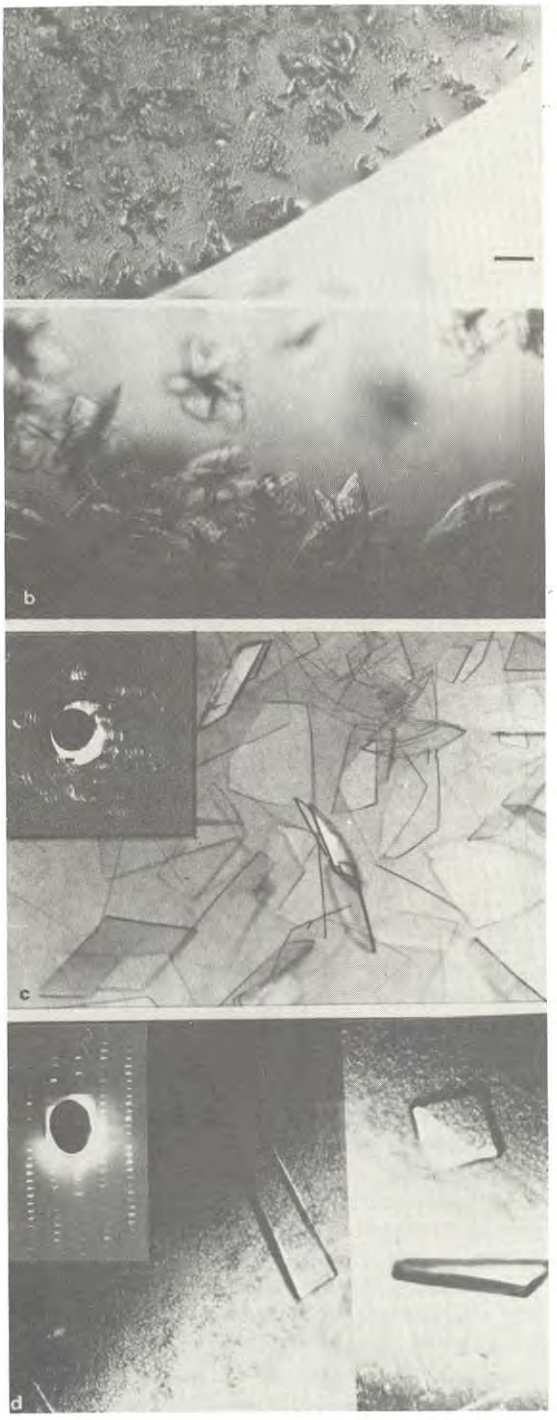

Figure 5. Growth of large, ordered three-dimensional crystals of the 50S ribosomal subunits from *H. marismortui* by vapor diffusion at 19°C (Bar length=0.2 mm). (*a*) Microcrystals obtained within 1–2 days. Droplets of 7–8% polyethylene glycol (PEG), 2.5 M KCl, 0.5 M NH_4Cl, 0.15–0.20 M $MgCl_2$, and 10 mM spermidine (pH 5.0–5.2) were equilibrated with 3.0 M KCl, 9% PEG, 0.5 M NH_4Cl, and 0.20 M $MgCl_2$. (*b*) Crystals obtained within 2–3 days in droplets containing lower KCl concentration than used in *a*. Droplet of 4–5% PEG, 1.2–1.7 M KCl, 0.5 M NH_4Cl, 0.10 M $MgCl_2$, and 10 mM spermidine were equilibrated with reservoirs as in *a*. (*c*) Crystals obtained within 3–5 days from droplets similar to those used for *b*, equilibrated with reservoirs of lower KCl concentrations. Droplet of 4–5% PEG, 1.2 M KCl, 0.5 M NH_4Cl, 0.05–0.10 M $MgCl_2$, and 10 mM spermidine (pH 5.0–5.6) were equilibrated with 1.7 M KCl, 9% PEG, 0.5 M NH_4Cl, and 0.10 M $MgCl_2$. An X-ray diffraction pattern taken perpendicular to the thin axis of the crystals, obtained under conditions similar to those described in Fig. 6, is inserted. (*d*) Crystals obtained by seeding of crystals from *c* in a crystallization drop containing 5% PEG, 1.2 M KCl, 0.5 M NH_4Cl, 0.03 M $MgCl_2$ (pH 5.6), which was equilibrated with 7% PEG, 1.7 M KCl, 0.5 M NH_4Cl, and 0.03 M $MgCl_2$ (pH 5.6). Seeds were small, well-shaped crystals, transferred into a stabilization solution of 7% PEG in 1.7 M KCl, 0.5 M NH_4Cl, and 0.05 M $MgCl_2$ (pH 5.6). An X-ray diffraction pattern taken perpendicular to the thin axis of the crystals, obtained under conditions described in Fig. 6, is inserted.

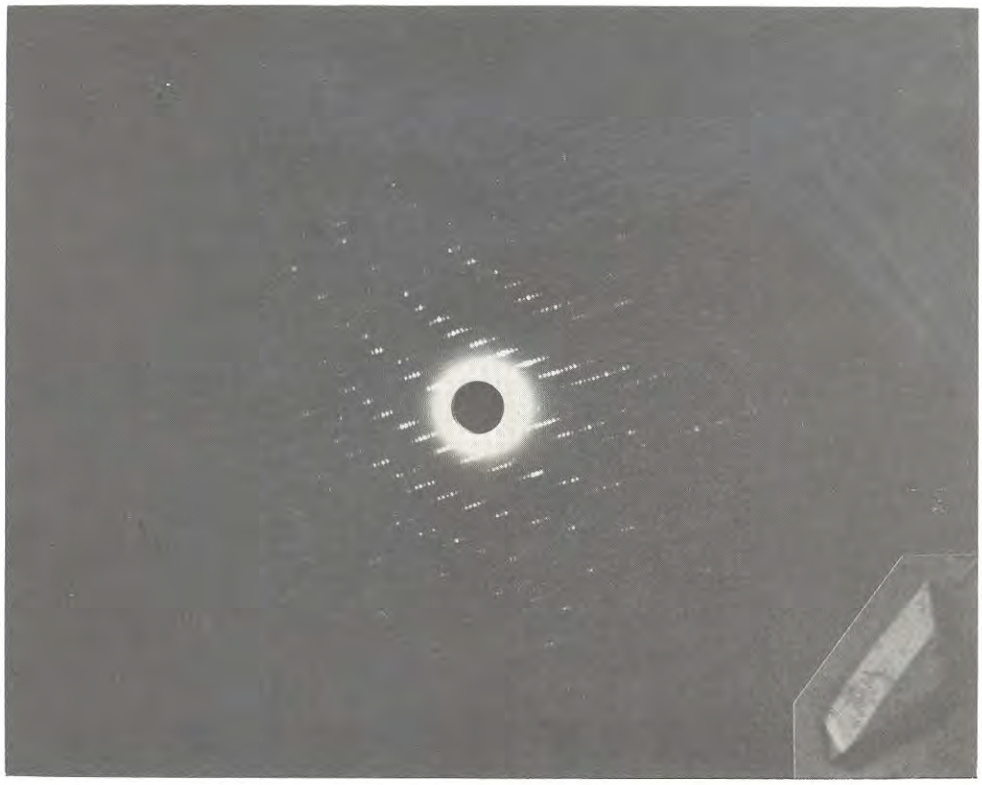

Figure 6. A 1° rotation pattern of a crystal similar to the inserted one. The pattern was obtained at −180°C with synchrotron radiation (7.1 station at SSRL). Wavelength, 1.54 Å; exposure time, 2 min; crystal to film distance, 135 mm. (*Insert*) A crystal of the 50S ribosomal subunits of *H. marismortui* obtained under similar conditions to Fig. 5 (*d*).

ture determination is hoped to be less dependent on the availability of synchrotron radiation.

Most recently we were able to obtain three-dimensional crystals from small (30S) ribosomal subunits from *Thermus thermophilus*. These have been grown at 4°C in X-ray capillaries, as described in Yonath et al. (1982b), using a mixture of ethylbutanol and ethanol at pH 8.3. Characterization of the crystal is currently underway.

Heavy-atom Derivatives

The most common method in protein crystallography to derive phases is multiple isomorphous replacement (MIR). For an object as large, asymmetric, and complex as the 50S ribosomal subunit, it is necessary to use extremely dense and compact compounds. Heavy-atom clusters are most suitable for this purpose.

An example of a suitable candidate for this purpose is a gold cluster, $Au_{11}(CN)_3(P[C_6H_4\text{-}p\text{-}CH_2NR]_3)_7$, of a molecular weight of about 5200 and in which the gold core has a diameter of 8.5 Å. Several variations of this cluster, prepared with phosphine ligands in which NR is a combination of NH_2, $NHCOCH_3$, and $N(COCH_3)$-CH_2CH_2OH (Fig. 7) have been prepared (S. Weinstein and W. Jahn, in prep.). The variants in which NR is either NH_2 or $N(COCH_3)CH_2CH_2OH$ or a mixture of these are soluble in the crystallization solution of 50S subunits from *H. marismortui*. One of these variants, with all $NR=NH_2$, was used for the formation of a heavy-atom derivative by soaking of native crystals in its solution. Crystallographic data (to 18 Å resolution) show isomorphous unit cell constants with observable differences in the intensities.

Because the surface of the ribosomal subunits is a composite of a variety of potential interaction sites, soaking in solutions of a heavy-atom cluster may give rise to multiple binding and complicate phase determination or make it impossible. Thus, in order to obtain usable heavy-atom derivatives, these clusters should preferably be covalently bound to one or a few specific sites on the ribosomal particles. This may be achieved by covalent binding of a suitable heavy-atom cluster with exposed chemically active groups of ribosomal proteins (e.g., —SH) or ends of rRNA on the intact particles prior to crystallization. Another possibility is to attach a heavy-atom cluster to tailor-made carriers that bind to specific sites on ribosomes or on ribosomal components that can then be reconstituted into the particles. To this end the following approaches were taken: First, free sulfhydryls on the surface of the 50S subunit have been located by reacting with radioactive *N*-ethylmaleimide. The binding sites were analyzed by locating radioactivity in two-dimensional gels of the ribosomal proteins. It was found that in the case of 50S subunits from *B. stearothermophilus* there are two proteins (L11 and L13) that definitely bind *N*-ethyl-

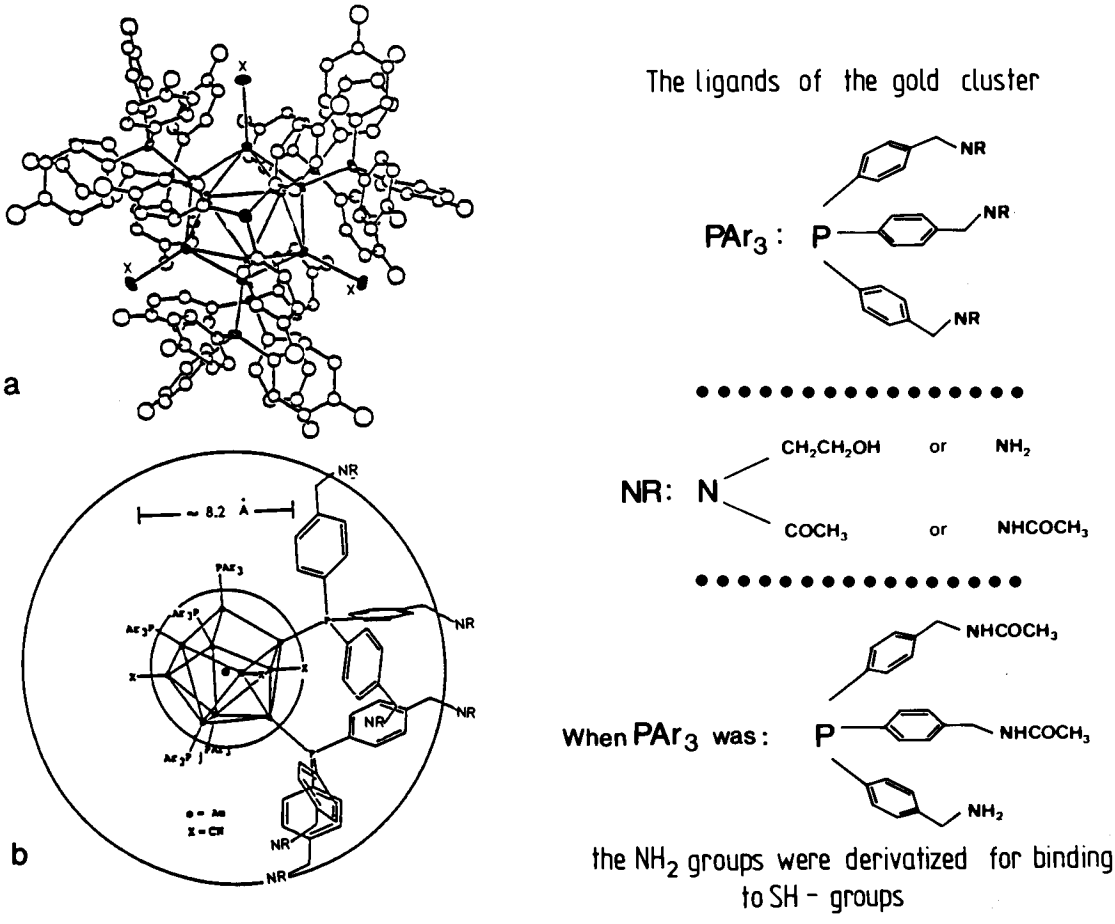

Figure 7. (*a*) Postulated molecular structure of $Au_{11}(CN)_3(P[C_6H_4\text{-}p\text{-}CH_2NR]_3)_7$ based on the crystal structure of $Au_{11}I_3(P[p\text{-}FC_6H_4]_3)_7$ (Bellon et al. 1972). (*b*) Semi-schematic presentation of $Au_{11}(CN)_3(P[C_6H_4\text{-}p\text{-}CH_2NR]_3)_7$ depicting the gold core of 8.2 Å diameter and the arrangement of the ligands around it (Wall et al. 1982).

maleimide. For *H. marismortui* most of the radioactivity was associated with one protein. Second,the gold cluster described above was prepared such that it could be bound to accessible —SH groups. Since this cluster is rather bulky, its accessibility was increased by the insertion of spacers, differing in length, to the cluster as well as to the free —SH groups on the ribosomal particles. Radioactive ^{14}C-labeling of this cluster as well as neutron activation analysis enabled us to determine the extent of the association of the cluster with the particles. The results of both analytical methods show that a spacer of minimum length of about 10 Å between the —SH group of a ribosomal protein and the N atom on the cluster is needed for significant binding. Furthermore, the extent of binding depends also on the structure of the spacer (S. Weinstein and W. Jahn, in prep.). Preliminary experiments indicate that the products of the derivatization reaction with 50S particles could be crystallized.

In parallel, a mutant of *B. stearothermophilus* that lacks protein L11 was obtained by growing cells in the presence of thiostrepton at 60°C. The 50S mutated ribosomal subunits crystallize in two and three dimensions under the same conditions as, and are isomorphous to, those obtained from the 50S ribosomal subunits of the wild type (Yonath et al. 1986a). This shows that L11, the missing protein, is not involved in crystal forces in the native crystals (in contrast, removal of protein L12 prevents crystallization). As mentioned above, *N*-ethylmaleimide binds to the —SH group of protein L11 on the ribosome particle. Furthermore, this binding does not reduce the activity and does not interfere with the crystallizability of the modified particles. Thus, modifying L11 with heavy-atom clusters is not expected to interfere with crystal packing and isomorphism. These observations open a new route for the preparation of specifically bound heavy atoms, by attaching clusters to the isolated protein, followed by reconstitution of the modified compound into the mutated particles.

Since protein L11 is believed to be nearly globular (Giri et al. 1984), its location may be determined in a Patterson electron density map with coefficients of $|F(wild)|\text{-}|F(mutant)|$, and may serve, by itself, as a super large heavy-atom derivative. At preliminary stages of structure determination, this approach may provide phase information and reveal the location of the missing protein.

CONCLUDING REMARKS

We have demonstrated here that diffraction methods can be employed for the determination of the three-dimensional structure of intact ribosomal particles. We expect that our studies, supported by biophysical, biochemical, and genetic knowledge, will yield a reliable model for the ribosome and lead to the understanding of the molecular mechanism of protein biosynthesis.

ACKNOWLEDGMENTS

We would like to thank Dr. H. Hope for introducing cryotemperature crystallography; Dr. W. Jahn for his involvement in the studies on the gold cluster; Drs. M.A. Saper, K.S. Bartels, F. Frolow, C. Kratky, and G. Weber for their efforts in data collection; Dr. F.L. Hirshfeld for his critical comments; Drs. J. Sussman and B. Shaanan for assisting us with computing and display problems; Dr. M. Shoham for his contribution to the crystallization process; Drs. K. Wilson, H.D. Bartunik, J. Helliwell, M. Papiz, K. Moffat, W. Schildcamp, P. Pizackerley, and E. Merrit for providing us with synchrotron radiation facilities; and I. Makowski, T. Arad, P. Webster, H.S. Gewitz, J. Piefke, J. Müssig, J. Halfon, C. Glotz, B. Romberg, G. Idan, and H. Danz for technical assistance. This work was supported by Bundesministerium für Forschung und Technologie (05 180 MP B0), National Institutes of Health (GM-34360), and Minerva research grants.

REFERENCES

Appelt, K., J. Dijk, R. Reinhardt, S. Sanhuesa, S.W. White, K.S. Wilson, and Y. Yonath. 1981. The crystallization of ribosomal proteins from the 50S subunit of the *Escherichia coli* and *Bacillus stearothermophilus* ribosome. *J. Biol. Chem.* **256:** 11787.

Arad, T., K.R. Leonard, H.G. Wittmann, and A. Yonath. 1984. Two-dimensional crystalline sheets of *Bacillus stearothermophilus* 50S ribosomal particles. *EMBO J.* **3:** 127.

Arad, T., J. Piefke, S. Weinstein, H.S. Gewitz, A. Yonath, and H.G. Wittmann. 1987a. Three-dimensional image reconstruction from ordered arrays of 70S ribosomes. *Biochimie* (in press).

Arad, T., J. Piefke, H.S. Gewitz, B. Romberg, C. Glotz, J. Müssig, A. Yonath, and H.G. Wittmann. 1987b. The growth of ordered two-dimensional sheets of ribosomal particles from salt-alcohol mixtures. *Anal. Biochem.* (in press).

Bartlett, P.A., B. Bauer, and S.J. Singer. 1978. Synthesis of water soluble undecagold cluster compounds of potential importance in electron microscopy and other studies of biological systems. *J. Amer. Chem. Soc.* **100:** 5085.

Bellon, P., M. Manassero, and M. Sansoni. 1972. Crystal and molecular structure of tri-iodoheptakis(tri-fluorophenylphosphine)undecagold. *J. Chem. Soc. (Dalton Trans.)* 1481.

Bernabeau, C. and J.A. Lake. 1982. Nascent polypeptide chains emerge from the exit domain of the large ribosomal subunit: Immune mapping of the nascent chain. *Proc. Natl. Acad. Sci.* **79:** 3111.

Blobel, G. and D.D. Sabatini. 1970. Controlled proteolysis of nascent polypeptides in rat liver cell fractions. *J. Cell Biol.* **45:** 130.

Chambliss, G., G.R. Craven, J. Davies, K. Davies, L. Kahan, and M. Nomura, eds. 1979. *Ribosomes: Structure, function, and genetics.* University Park Press, Baltimore.

Giri, L., W.E. Hill, H.G. Wittmann, and B. Wittmann-Liebold. 1984. Ribosomal proteins: Their structure and spatial arrangements in prokaryotic ribosomes. *Adv. Protein Chem.* **36:** 1.

Hardesty, B. and G. Kramer, eds.. 1986. *Structure, function, and genetics of ribosomes.* Springer-Verlag, Heidelberg.

Hogle, J.M. 1982. Preliminary studies of crystals of poliovirus type I. *J. Mol. Biol.* **160:** 663.

Hope, H. 1985. New techniques for handling of air-sensitive crystals. In *American Crystal Association Abstracts*, Ser. 2, vol. 13, abstract PA3.

Klug, A., K.C. Holmes, and J.T. Finch. 1961. X-ray diffraction studies on ribosomes from various sources. *J. Mol. Biol.* **3:** 87.

Langridge, R. and K.C. Holmes. 1962. X-ray diffraction studies of concentrated gels of ribosomes from *E. coli*. *J. Mol. Biol.* **5:** 611.

Leijonmarck, M., S. Eriksson, and A. Liljas. 1980. Crystal structure of a ribosomal component at 2.6 Å resolution. *Nature* **286:** 824.

Leonard, K.R., T. Arad, B. Tesche, V.A. Erdmann, H.G. Wittmann, and A. Yonath. 1982. Crystallization, electron microscopy and three-dimensional reconstitution studies of ribosomal subunits. In *Electron microscopy 1982*, vol. 3, p. 9. Offizin Paul Hartung, Hamburg.

Makowski, I., F. Frolow, M.A. Saper, M. Shoham, H.G. Wittmann, and A. Yonath. 1987. Single crystals of large ribosomal particles from *Halobacterium marismortui* diffract to 6 Å. *J. Mol. Biol.* **193:** 819.

Malkin, L.I. and A. Rich. 1967. Partial resistance of nascent polypeptide chains to proteolytic digestion due to ribosomal shielding. *J. Mol. Biol.* **26:** 329.

Matthews, B.W. 1968. Solvent content of protein crystals. *J. Mol. Biol.* **33:** 491.

Milligan, R.A. and P.N.T. Unwin. 1986. Location of exit channel for nascent protein in 80S ribosomes. *Nature* **319:** 693.

Nierhaus, K.H. and H.G. Wittmann. 1980. Ribosomal function and its inhibition by antibiotics in prokaryotes. *Naturwissenschaften* **67:** 234.

Piefke, J., T. Arad, H.S. Gewitz, A. Yonath, and H.G. Wittmann. 1986. The growth of ordered two-dimensional sheets of 70S ribosomes from *Bacillus stearothermophilus*. *FEBS Lett.* **209:** 104.

Richmond, T., J.T. Finch, B. Rushton, D. Rhodes, and A. Klug. 1984. Structure of the nucleosome core particle at 7 Å resolution. *Nature* **311:** 533.

Shevack, A., H.S. Gewitz, B. Hennemann, A. Yonath, and H.G. Wittmann. 1985. Characterization and crystallization of ribosomal particles from *Halobacterium marismortui*. *FEBS Lett.* **184:** 68.

Shoham, M., J. Müssig, A. Shevack, T. Arad, H.G. Wittmann, and A. Yonath. 1986. A new crystal form of the large ribosomal subunits from *Halobacterium marismortui*. *FEBS Lett.* **208:** 321.

Smith, W.P., P.C. Tai, and B.D. Davis. 1978. Interaction of secreted nascent chains with surrounding membrane in *Bacillus subtilis*. *Proc. Natl. Acad. Sci.* **75:** 5922.

Verschoor, A., J. Frank, and M. Boublik. 1985. Investigation of the 50S ribosomal subunit by electron microscopy and image analysis. *J. Ultrastruct. Res.* **92:** 180.

Wall, J.S., J.F. Hainfeld, P.A. Bartlett, and S.J. Singer. 1982. Observation of an undecagold cluster compound in the scanning transmission electron microscope. *Ultramicroscopy* **8:** 397.

Wilson, K.S., K. Appelt, J. Badger, I. Tanaka, and S.W. White. 1986. Crystal structure of a prokaryotic ribosomal protein. *Proc. Natl. Acad. Sci.* **83:** 7251.

Wittmann, H.G. 1982. Components of bacterial ribosomes. *Annu. Rev. Biochem.* **51:** 155.

———. 1983. Architecture of prokaryotic ribosomes. *Annu. Rev. Biochem.* **52:** 35.

Wittmann, H.G. and A. Yonath. 1985. Diffraction studies on crystals of ribosomal particles. In *The structure and function of the genetic apparatus* (ed. C. Nicolini and P.O.P. Ts'o), p. 177. Plenum Press, New York.

Wittmann, H.G., J. Müssig, H.S. Gewitz, J. Piefke, H.J. Rheinberger, and A. Yonath. 1982. Crystallization of *Escherichia coli* ribosomes. *FEBS Lett.* **146:** 217.

Yonath, A. 1984. Three-dimensional crystals of ribosomal particles. *Trends Biochem. Sci.* **9:** 227.

Yonath, A. and H.G. Wittmann. 1987a. Crystallographic and image reconstruction studies on ribosomal particles from bacterial sources. *Methods Enzymol.* (in press).

———. 1987b. Crystallographic and image reconstruction studies on ribosomes. In *Modern methods in protein chemistry* (ed. H. Tschesche). W. de Gruyter-Verlag, Berlin. (In press.)

———. 1987c. Towards a molecular model for the large ribosomal particle. In *Molecular structures, biological activity and chemical reactivity* (ed. J. Stezowski). Oxford Press, England. (In press.)

Yonath, A., K.R. Leonard, and H.G. Wittmann. 1987. A tunnel in the large ribosomal subunit revealed by three-dimensional image reconstruction. *Science* **236:** 813.

Yonath, A., J. Müssig, and H.G. Wittmann. 1982a. Parameters of crystal growth of ribosomal subunits. *J. Cell. Biochem.* **19:** 145.

Yonath, A., M.A. Saper, and H.G. Wittmann. 1986a. Studies on crystals of intact ribosomal particles. In *Structure, function, and genetics of ribosomes* (ed. B. Hardesty and G. Kramer), p. 112. Springer-Verlag, Heidelberg.

Yonath, A., H.D. Bartunik, K.S. Bartels, and H.G. Wittmann. 1984. Some X-ray diffraction pattern from single crystals of the large ribosomal subunit from *Bacillus stearothermophilus*. *J. Mol. Biol.* **177:** 201.

Yonath, A., J. Piefke, J. Müssig, H.S. Gewitz, and H.G. Wittmann. 1983a. A compact three-dimensional crystal form of the large ribosomal subunit from *Bacillus stearothermophilus*. *FEBS Lett.* **163:** 69.

Yonath, A., M.A. Saper, F. Frolow, I. Makowski, and H.G. Wittmann. 1986b. Characterization of single crystals of the large ribosomal particles from a mutant of *Bacillus stearothermophilus*. *J. Mol. Biol.* **192:** 161.

Yonath, A., J. Müssig, B. Tesche, S. Lorenz, V.A. Erdmann, and H.G. Wittmann. 1980. Crystallization of the large ribosomal subunits from *Bacillus stearothermophilus*. *Biochem. Int.* **1:** 428.

Yonath, A., B. Tesche, S. Lorenz, J. Müssig, V.A. Erdmann, and H.G. Wittmann. 1983b. Several crystal forms of the *Bacillus stearothermophilus* 50S ribosomal particles. *FEBS Lett.* **154:** 15.

Yonath, A., G. Khavitch, B. Tesche, J. Müssig, S. Lorenz, V.A. Erdmann, and H.G. Wittmann. 1982b. The nucleation of crystals of the large ribosomal subunit from *Bacillus stearothermophilus*. *Biochem. Int.* **5:** 629.

Yonath, A., M.A. Saper, I. Makowski, J. Müssig, J. Piefke, H.D. Bartunik, K.S. Bartels, and H.G. Wittmann. 1986c. Characterization of single crystals of the large ribosomal particles from *Bacillus stearothermophilus*. *J. Mol. Biol.* **187:** 633.